Correlation of open-circuit voltage and energy levels in zinc-phthalocyanine: C_{60} bulk heterojunction solar cells with varied mixing ratio

Max L. Tietze,[*] Wolfgang Tress, Steffen Pfützner, Christoph Schünemann, Lorenzo Burtone, Moritz Riede,[†] and Karl Leo[‡]
Institut für Angewandte Photophysik, Technische Universität Dresden, 01062 Dresden, Germany

Koen Vandewal
Department of Materials Science and Engineering, Stanford University, Stanford, California 94305, USA

Selina Olthof,[§] Philip Schulz, and Antoine Kahn
Department of Electrical Engineering, Princeton University, Princeton, New Jersey 08544, USA
(Received 10 April 2013; revised manuscript received 4 July 2013; published 20 August 2013)

The maximum open-circuit voltage V_{OC} of bulk-heterojunction solar cells is limited by the effective HOMO(donor)-LUMO(acceptor) gap of the photoactive absorber blend. We investigate blend layers comprising zinc-phthalocyanine (ZnPc) and the buckminster fullerene C_{60} with ultraviolet, x-ray, and inverse photoelectron spectroscopy. By varying the volume mixing ratio ZnPc:C_{60} from 6:1 to 1:6, we observe a linear increase of the HOMO(ZnPc)-LUMO(C_{60}) gap by 0.25 eV. The trend in this gap correlates with the change in the charge transfer energy measured by Fourier-transform photocurrent spectroscopy as well as with the observed open-circuit voltage of solar cells containing ZnPc:C_{60} as the photoactive absorber layer. Furthermore, the morphology of different ZnPc:C_{60} blend layers is investigated by grazing-incidence x-ray diffraction. As physical origins for the changed energy levels, a suppressed crystallization of the C_{60} phase in the presence of donor molecules as well as concentration-dependent growth modes of the ZnPc phase are suggested.

DOI: 10.1103/PhysRevB.88.085119 PACS number(s): 79.60.Fr, 88.40.jr, 61.05.cf

I. INTRODUCTION

The performance of organic solar cells has rapidly been improved over the last decade, reaching most recently a record power conversion efficiency η_{PCE} of 12.0%.[1] A key concept that has enabled this development is the application of blends of donor and acceptor molecules as photoactive absorber layers in so-called bulk heterojunctions (BHJs),[2] because they facilitate significantly enhanced photocurrents if percolation of electrons on the acceptor and holes on the donor phase to the contacts is guaranteed.[3] Hereby, the maximum achievable open-circuit voltage V_{OC}, which is ideally determined by splitting of the electron and hole quasi-Fermi-levels,[4] is limited by the effective gap V_0 between the highest occupied molecular orbital (HOMO) of the donor and the lowest unoccupied molecular orbital (LUMO) of the acceptor. However, typically lower values than V_0 are measured for eV_{OC} (e: elementary charge) which still limits the overall η_{PCE}. Thus, for further improvement of η_{PCE} a deeper understanding of the physical processes which determine V_{OC} is required.

Tress *et al.*[5] reported on an improvement of V_{OC} of ZnPc:C_{60} bulk heterojunction solar cells from 0.54 V to 0.62 V by decreasing the volume mixing ratio from 2:1 to 1:3. This trend in V_{OC} was shown to be independent of the hole transport layer that served as hole contact. Therefore, Tress *et al.* concluded that the change in V_{OC} is caused by the ZnPc:C_{60} active layer itself, where either a change in energy levels or a modified recombination probability were discussed as reasons. By comparing numerical simulations of devices with different hole transport layers, the authors concluded that a shift in the ionization energy (IE) of ZnPc upon blending it with C_{60} is the most likely reason.

Changes in the energy levels of the donor or acceptor material upon changing the blend stoichiometry have been previously reported in polymer:fullerene solar cells. It has been argued that increased ordering of the fullerene lowers its IE.[6,7] Energetic differences between crystalline and amorphous phases further have been proposed to assist in the initial charge separation process. Additionally, changes in the overall dielectric constant of the blend were proposed to influence the energetics.[8]

Park *et al.*[9] investigated the energy level alignment of the interfaces ZnPc/C_{60} and ZnPc/ZnPc:C_{60}(1:1)/C_{60} by ultraviolet photoelectron spectroscopy (UPS). They report on a larger HOMO(ZnPc)-LUMO(C_{60}) gap within the blend (1.04 eV) compared to the flat interface (0.75 eV). However, a systematic quantitative explanation and correlation between V_{OC} of a ZnPc:C_{60} bulk heterojunction solar cell and the blend energy level alignment remains still open.

In this article, we investigate the energy levels of ZnPc and C_{60} within blend layers by means of UPS and inverse photoemission spectroscopy (IPES) varying the volume mixing ratio (1:6, 1:3, 1:1, 3:1, 6:1). We can attribute the improved V_{OC} for higher C_{60} content to an enlarged effective HOMO(ZnPc)-LUMO(C_{60}) gap. Additionally, measurements of the charge-transfer state energy E_{CT} by Fourier-transform photocurrent spectroscopy (FTPS) reveal an increase of E_{CT} with rising C_{60} amount in the blend. Since measurements of the permittivity of ZnPc:C_{60} mixed layers by capacitance-voltage spectroscopy show no clear trend, we attribute the shifts in the energy levels to morphological changes. By grazing-incidence x-ray diffraction measurements we found that the nanocrystallinity of the C_{60} phase is disturbed by the ZnPc molecules for acceptor concentrations below 75 vol.%. A correlation to the UPS results suggests this to be the main origin for the mixing ratio dependence of V_{OC}.

II. THEORY

The V_{OC} of an organic bulk heterojunction (BHJ) solar cell is determined by the quasi-Fermi-level splitting of the electrons on the acceptor and the holes on the donor phase, as long as no injection or extraction barriers are present.[10] Assuming proportionality between the photocurrent and the illumination intensity I, the dependence of V_{OC} on the temperature T and intensity I can generally be expressed as

$$eV_{OC} = V_0 + k_B T \ln\left(\frac{I}{I_0}\right). \quad (1)$$

Here, V_0 and I_0 are device-specific parameters. The maximum achievable open-circuit voltage is given by $eV_{OC} \xrightarrow{T\to 0} V_0$. In the literature, V_0 is commonly regarded as the effective gap of the donor-acceptor blend, i.e., $V_0 = -\mathrm{HOMO}_{\mathrm{donor}} + \mathrm{LUMO}_{\mathrm{acceptor}}$,[11] or as the difference between the donor ionization energy and the acceptor electron affinity, $V_0 = \mathrm{IE}_{\mathrm{donor}} - \mathrm{EA}_{\mathrm{acceptor}}$.[12] Most recently, these relations have been confirmed for small molecule bulk heterojunction solar cells containing C_{60} as acceptor mixed with various donor materials.[13,14]

However, Vandewal *et al.* suggested identifying V_0 with the energy of the charge-transfer (CT) state E_{CT} at the donor-acceptor interface.[15] A good correspondence between V_0 and E_{CT} was found, with E_{CT} determined from the low-energy part of the spectral region of weak CT absorption of the photovoltaic external quantum efficiency EQE_{PV}[15]

$$EQE_{PV}(E) \sim \frac{1}{E\sqrt{4\pi\lambda k_B T}} \exp\left[-\frac{(E_{CT}+\lambda-E)^2}{4\lambda k_B T}\right]. \quad (2)$$

Here, E_{CT} is the energy difference between the CT complex ground state and lowest energy (excited) CT state. λ indicates the according vibronic reorganization energy of the CT absorption process. Thus, E_{CT} can directly be obtained from the low-energy part of the $EQE_{PV}(E)$ spectrum, if measured with a sufficiently high sensitive technique, e.g., FTPS,[15] able to spectrally resolve the CT absorption band.

III. EXPERIMENTAL

The UPS and x-ray photoelectron spectroscopy (XPS) samples are thermally evaporated at room temperature under high-vacuum conditions (base pressure $< 1 \times 10^{-8}$ mbar). The materials ZnPc (TCI Europe, Belgium) and C_{60} (CreaPhys, Germany) are of sublimed purity grade. Mixed layers are obtained by co-evaporation of both materials controlling the blend ratio, i.e., evaporation rates, with two independent quartz crystal microbalances. As substrates for the UPS/XPS samples, sputter-cleaned silver foils (99.995%, MaTecK, Juelich, Germany) covered with 30 nm thermally evaporated gold are used. The UPS/XPS experiments are performed with a Phoibos 100 system (Specs, Berlin, Germany) at a base pressure of 1×10^{-10} mbar directly connected to the evaporation tool. For UPS (He I, 21.22 eV, sample bias -8 V) the energy resolution is 130 meV and for XPS (Al K_α, 1486.6 eV) 400 meV, respectively. The experimental error (reproducibility) is estimated to be 50 meV for both methods. For each UPS spectrum the high binding energy cutoff E_{HBEC} (HBEC) as well as the HOMO onset of the occupied states E_{HOMO} are determined. Hence, the film work function is given by $\mathrm{Wf} = 21.22\ \mathrm{eV} - E_{HBEC}$ and the ionization energy by $\mathrm{IE} = \mathrm{Wf} + E_{HOMO}$. All UPS/XPS measurements are performed in the dark to avoid any absorption and thus exciton dissociation effects resulting in increased free charge carrier concentrations in both materials. However, since the UV source is not monochromatic and emitting also weakly in the visible spectrum, such illumination effects cannot be completely excluded, but should be negligible in comparison to illumination with 1 sun intensity (1000 W/m^2).

Additional photoelectron spectroscopy measurements for the determination of the transport gap were performed at Princeton University using a standard UPS setup with HeI excitation at an energy resolution of 150 meV in combination with an inverse photoelectron spectrometer (IPES) setup. The IPES experiment is performed in the isochromat mode at an energy resolution of 400 meV using a setup described elsewhere.[16] The materials ZnPc and C_{60} (both from Sigma Aldrich) are used as received and are evaporated onto sputter-cleaned gold foil (Surepure Chemetals).

The actual mixing ratios of the UPS/IPES samples are confirmed by XPS by scanning C1*s* and Zn2*p*. The carbon peak contains signal from C_{60} and ZnPc as well and thus we fit the C1*s* blend peak with C1*s* subpeaks obtained from pure C_{60} and ZnPc layers. Accordingly, the blend molar ratio is calculated by the intensity ratios C1*s* (C_{60})/C1*s* (ZnPc) and/or C1*s* (C_{60})/Zn2*p* (ZnPc) taking the different cross sections and atom numbers per molecule into account. Subsequently, the actual volume mixing ratios (vol.%) are deduced. Unless stated otherwise, the mixing ratios are given by (*X*:*Y*) which is equal to the weight ratio, i.e., to the intended rate ratio during evaporation.

The solar cells are fabricated in a custom-made vacuum evaporation tool (K. J. Lesker, UK) at a base pressure of 1×10^{-8} mbar. As substrates prestructured and ultrasonic bath (detergent, acetone, ethanol, and isopropanol) cleaned ITO-coated glasses (Thin Film Devices, US) are used. The dopants used in the transport layers are purchased from Novaled AG, Dresden (NDP2), and from MTR Ltd., US ($C_{60}F_{36}$). *IV* measurements are performed at room temperature under simulated sunlight (16S-150 V.3 by Solar Light Co., USA) with an assumed spectral mismatch of 0.79 for all solar cells. The actual mismatch factors of the solar cells with varied blend ratios are in between 0.764...0.799, which results in a variation of the effective illumination intensity by a maximum of 3.5%. Its error impact on V_{OC} is estimated by Eq. (1) to be <1 mV and hence negligible. Since the fill factors of the investigated solar cells are higher than 46% (see Supplemental Material[18]), the dominant error contribution to determination of V_{OC} is due to interpolation of the *j*-*V* characteristics to $j = 0$, and estimated to ± 7 mV.

For the highly sensitive *EQE* measurements by FTPS, a Vertex 70 FTIR from Bruker, equipped with a QTH lamp, quartz beamsplitter, and external detector is used. Photovoltaic devices are illuminated by the FTIRs modulated output light beam. A low noise current amplifier (SR570) is used to amplify the photocurrent. The output signal of the current amplifier is fed back into the external detector port of the FTIR, enabling collecting of the photocurrent spectrum.

The capacitance measurements are performed in the dark with an Autolab PGSTAT302N. The probe signal has an amplitude of 10 mV (rms) and the bias signal is varied from 0.5 V to −1.0 V. The probe signal frequency is varied from 10 Hz to 1 MHz and the impedance spectra are then fitted for estimation of the device capacitance.

Grazing-incidence x-ray diffraction experiments are performed by an Bruker D8 Discover diffractometer using Cu $K_{\alpha 1}$ irradiation. The incident angle is kept fixed at $\omega = 0.20^\circ$ whereas the detection angle θ is varied in 2θ steps of 0.1°. Further details of the experimental grazing-incidence x-ray diffraction (GIXRD) setup and the measurement procedure are described elsewhere.[17]

IV. RESULTS AND DISCUSSION

A. BHJ solar cells with varied mixing ratios

The ZnPc:C_{60} BHJ blend as absorber layer is sandwiched between an electron transport layer (C_{60}) and a *p*-doped hole transport layer (NDP9:Di-NPD, 5 wt.%) in a so-called p-i-i-metal device (cf. inset Fig. 1). Hereby, well-injecting contacts as well as a decreased probability of surface recombination are guaranteed by the doped HTL and the C_{60}/BPhen layer.

In Fig. 1 the V_{OC} of ZnPc:C_{60} BHJ solar cells with varying volume mixing ratios of C_{60} from 14 vol.% (6:1) to 86 vol.% (1:6) are shown. Increasing the C_{60} amount from 33 vol.% improves V_{OC} linearly by 0.1 V up to 0.63 V at 83 vol.%. Interestingly, V_{OC} also increases slightly for lower concentrations of C_{60}. The characteristic solar cell parameters such as the short-circuit current J_{SC} as well as the fill factor FF differ for the various C_{60} concentrations (not shown here; see Supplemental Material[18]). The change in FF from 51.7% to 45.8% by comparing the 2:1 and 1:6 sample reflects the charge transport properties of the blend.[19] Due to different absorption and/or recombination probability in the blend layers for different mixing ratios, the different photocurrents are expected to impede an unambiguous comparison of V_{OC}, since the second term of Eq. (1) is not constant. However, values for the short-circuit current density J_{SC} are in the range of 7.64 mA/cm^2 (1:1) to 4.58 mA/cm^2 (1:6), which is mainly caused by different absorption of the D:A blends. By using Eq. (1) and assuming $I_{eff} \propto J_{SC}$, we estimate that the absolute influence of the different photocurrents on V_{OC} has to be below 14 mV, i.e., significantly lower than the observed variation upon changes in the mixing ratio.

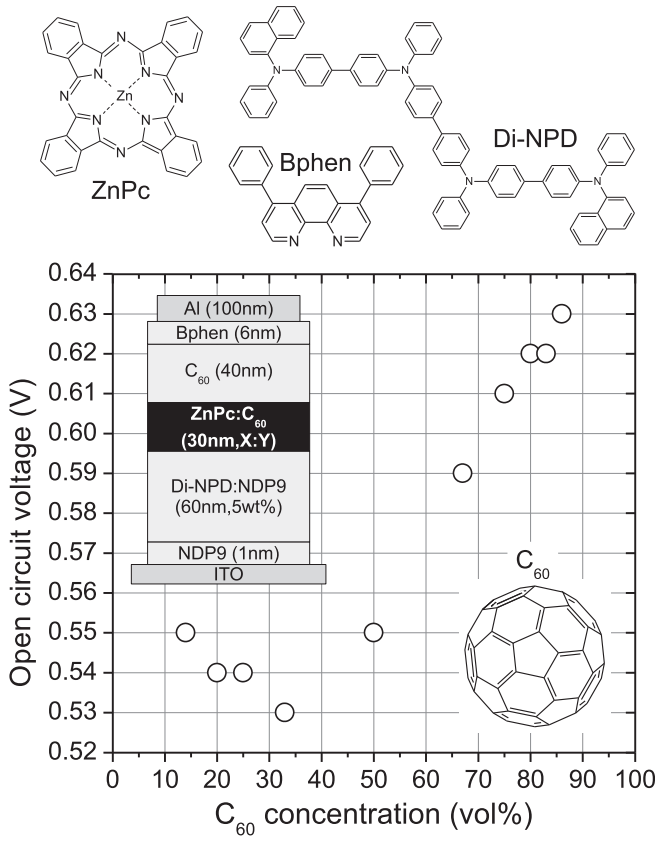

FIG. 1. Open-circuit voltage V_{OC} of pii-BHJ solar cells as a function of the ZnPc:C_{60} mixing ratio. The device structure is shown in the inset of the graph and the chemical structures of the employed molecules above.

In addition to theses estimations, Tress *et al.* measured V_{OC} for different mixing ratios under adjusted illumination intensities and therefore equal J_{SC} using either monochromatic blue or red LEDs.[5] They found that the observed difference in V_{OC} cannot be explained by different charge carrier densities. Also a changed recombination has been excluded by comparison to drift-diffusion simulations.[5] Hence, the observed variations in V_{OC} have to be attributed to changed effective gaps V_0 of the ZnPc:C_{60} blends of different mixing ratios, i.e., to a change in the energy levels of ZnPc and/or C_{60} upon blending both materials.

B. UPS/IPES measurements on ZnPc:C_{60} blends

To investigate the idea of an energy level shift being responsible for the observed changes in V_{OC}, we prepare UPS samples with 15 nm thick mixed layers and varying mixing ratios on a gold substrate. The high binding energy cutoff (HBEC) and the highest occupied molecular orbital (HOMO) region of the UPS spectra (subtracted secondary lines) of the 1:6, 1:1, and 6:1 samples are shown in Fig. 2 (gray circles). The spectra contain superimposed features of C_{60} and ZnPc. For determining the HOMO onsets of both materials within the blend, we fit the spectra with Gaussian peaks representing either C_{60} or ZnPc assuming a Touggard-type background (dotted line). The underlying subspectra of C_{60} (dashed-dotted lines) and ZnPc (dashed lines) are fitted from intrinsic reference samples (15 nm on Au) using Gaussian distributions (C_{60}: 4 peaks, ZnPc: 6 peaks). For fitting a blend layer spectrum these peaks are set fixed in their energetic distances and relative intensities for each material. The resulting overall fits (black lines) agree very well with the UPS data of the corresponding mixed layers. Slight deviations are only present for binding energies >3 eV. We attribute these deviations to changes in the secondary electron background of the blend layers compared to the pure film spectra, i.e., to a different increase of the Touggard-type background at higher binding energies for blends and intrinsic films. Since the spectra of the mixed films are fitted by rigid pure film subspectra, these differences are not considered by the applied fitting procedure. However, for low binding

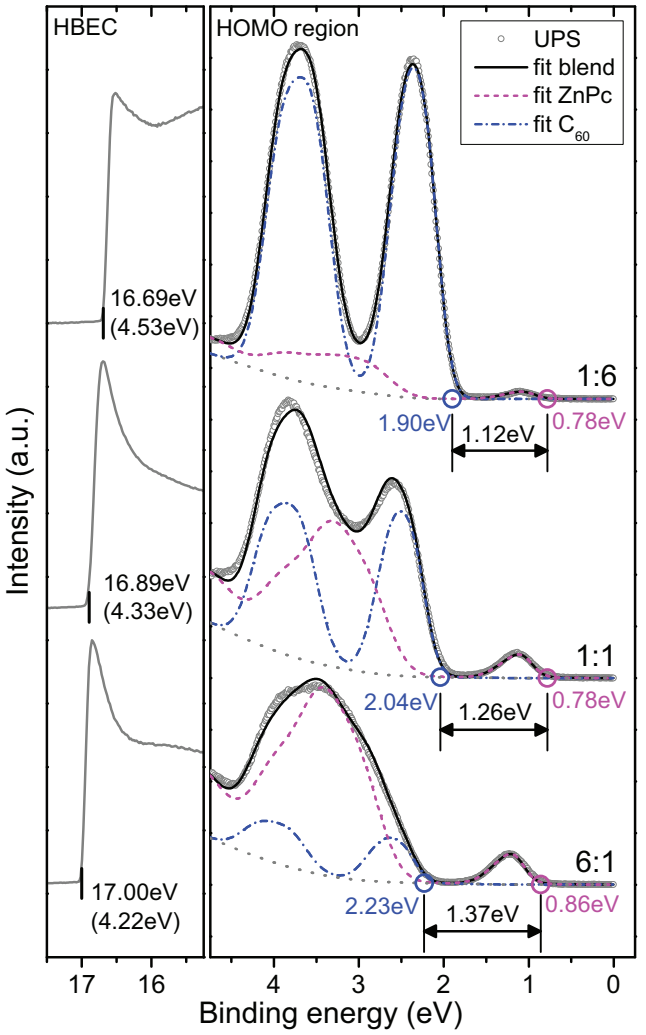

FIG. 2. (Color online) High binding energy cutoff (HBEC) and highest occupied molecular orbital (HOMO) region of the UPS spectra of 15 nm ZnPc:C_{60} (1:6, 1:1, and 6:1 volume mixing ratios) layers on gold. For determining the HOMO onsets of both materials within the blend layer, the mixed layer spectrum is fitted by subspectra (dashed-dotted: C_{60}, dashed: ZnPc) originally obtained from separate intrinsic reference samples. For the different mixing ratios the C_{60} and ZnPc subspectra are adapted in intensity. The obtained HOMO onsets are indicated by circles. The dotted gray lines represent assumed Touggard-type backgrounds.

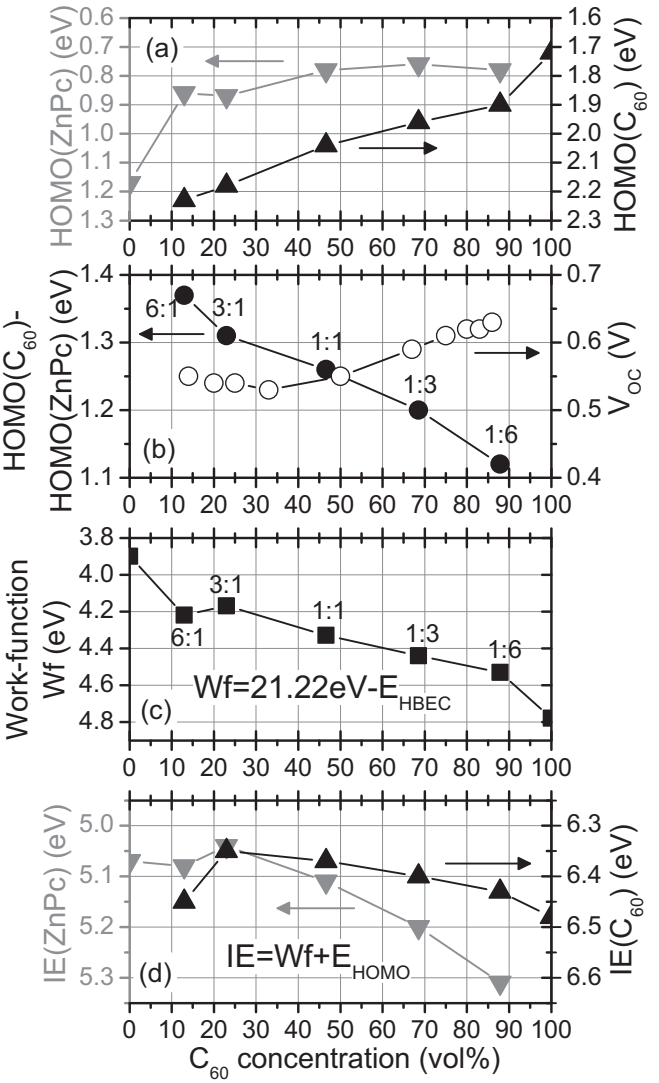

FIG. 3. (a) ZnPc and C_{60} HOMO onset values within mixed thin films determined by fitting UPS spectra (Fig. 2) as functions of the mixing concentration. (b) Corresponding HOMO(C_{60})-HOMO(ZnPc) difference in comparison to V_{OC} of respective BHJ solar cells. (c) Work function and (d) resulting individual IEs of ZnPc and C_{60} determined by the corresponding HOMO onsets.

energies <3 eV the secondary electron background is less important, wherefore the fitting yields excellent agreement with the measured blend spectra and allows for an exact determination of the respective HOMO-onset values. The obtained HOMO onsets are indicated by blue (C_{60}) and magenta (ZnPc) circles in Fig. 2.

This procedure was done for samples with intended ZnPc:C_{60} volume mixing ratios of 1:6, 1:3, 1:1, 3:1, and 6:1. The determined HOMO onsets of both materials within the blends as functions of the C_{60} amount as well as the layer work functions are summarized in Figs. 3(a) and 3(c). Mixing 14 vol.% C_{60} into ZnPc (6:1 sample in Fig. 2) reduces the HOMO onset of ZnPc from 1.17 eV (intrinsic on Au) to 0.86 eV. Higher C_{60} amounts are shifting the ZnPc HOMO onset by only less than 0.1 eV further towards the Fermi level. In the case of C_{60}, the HOMO onset linearly shifts to higher binding energies with decreasing C_{60} concentration from 1.90 eV (86 vol.%, 1:6) to 2.23 eV (14 vol.%, 6:1). This result is remarkable, because it suggests that C_{60} seems to get weakly *n*-type (electron affinity EA = 4.0 eV,[20] IE − EA = 2.4 eV) upon blending it with ZnPc. In contrast, the HOMO onset of ZnPc remains nearly unchanged with respect to the common Fermi level over a wide range of mixing ratios. These findings imply a decreased HOMO(C_{60})-HOMO(ZnPc) difference for higher C_{60} concentrations, which is indicated by the black arrows in Fig. 2 and plotted in Fig. 3(b). The values are scaling linearly with the C_{60} concentration from 1.37 eV (6:1) to 1.12 eV (1:6). Hence, by assuming a rigid HOMO-LUMO gap independent of the mixing ratio for at least C_{60}, the effective donor-acceptor gap V_0 must similarly increase with

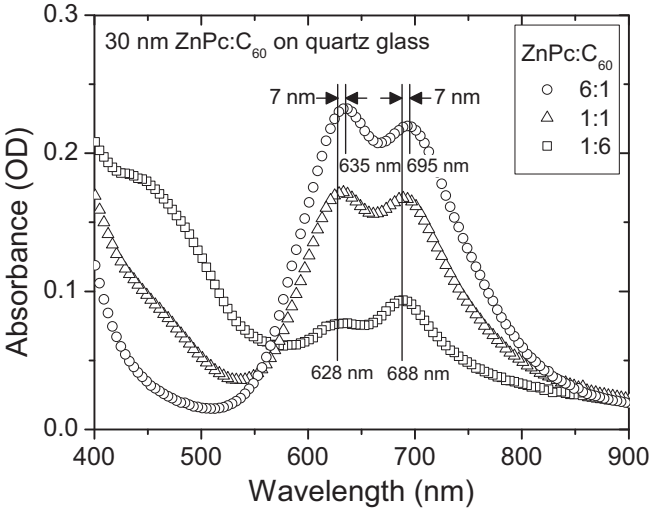

FIG. 4. Absorption spectra of 30 nm ZnPc:C_{60} blends with different mixing ratios evaporated on quartz glass.

increasing C_{60} amount by 0.25 eV, which qualitatively explains the observed V_{OC} dependence on the mixing ratio.

However, assuming a rigid individual HOMO-LUMO gap of C_{60} (and ZnPc) is not obvious, because different mixing ratios might change the polarization effect on individual molecules contained in different blends. In particular, the HOMO-LUMO gaps might be changed in comparison to the respective pure thin films. Hence, absorption as well as independent IPES measurements on different ZnPc:C_{60} blends are performed for studying the dependence of the individual optical and electrical gaps on the mixing ratio.

Absorption spectra of 1:6, 1:1, and 6:1 blends are shown in Fig. 4. The characteristic absorption bands of ZnPc are shifting by only 7 nm towards higher wavelengths upon increasing the ZnPc:C_{60} ratio from 1:6 to 6:1. Hereby, the shift from 688 nm (1.802 eV) to 695 nm (1.784 eV) corresponds to an energy difference of only 0.018 eV which suggest a nearly constant optical gap for ZnPc within all blends. Due to the relatively low absorption, a similar conclusion cannot reliably be drawn for C_{60}.

IPES and further UPS spectra of 1:1.4 and 2.2:1 blends are plotted in Fig. 5. In contrast to the optical gaps, the IPES measurements reveal varying individual electronic gaps for both materials. Comparing all four samples in Fig. 5, the ZnPc gap varies by 0.08 eV and the C_{60} gap by 0.17 eV, but without any clear trend on the mixing ratio. However, the already observed trend in the effective HOMO(ZnPc)-LUMO(C_{60}) gap is also reproduced here. Changing the ZnPc:C_{60} ratio from 2.2:1 to 1:1.43 increases the effective gap by ≈0.1 eV from 0.95 eV to 1.04 eV. Due to the low signal-to-noise ratio of IPES, further experiments on lower (higher) mixing ratios are unreliable, because an unambiguous fitting of the subspectra and thus determination of the characteristic LUMO onsets cannot be guaranteed. It shall be further emphasized that the measured changes in the electronic gaps are lower than the experimental energy resolution of IPES (400 meV), wherefore trends in the individual gaps cannot clearly be concluded on the scale of a few 10 meV. However, the former UPS results strongly suggest that the dependence of V_{OC} on the mixing

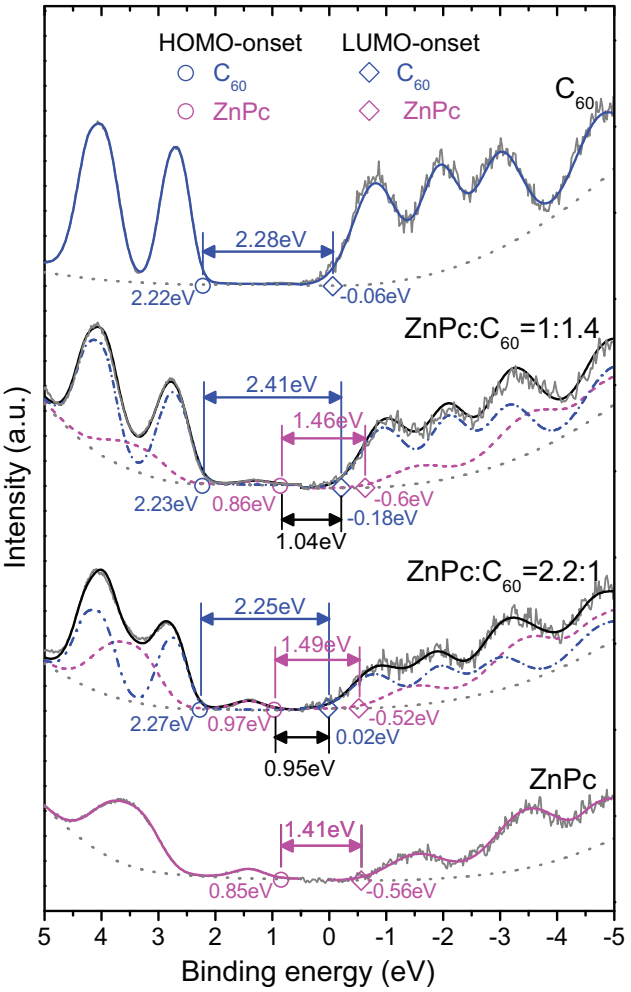

FIG. 5. (Color online) IPES and UPS spectra of pure ZnPc and C_{60} films as well as of 1:1.4 and 2.2:1 blends on gold. Mixed-layer spectra are fitted by subspectra (dashed-dotted: C_{60}, dashed: ZnPc) originally obtained from the intrinsic reference samples. The HOMO (LUMO) onsets of both materials are indicated by colored circles (diamonds). The dotted gray lines represent assumed Touggard-type backgrounds.

ratio can be attributed to shifting energy levels, since the HOMO(C_{60})-HOMO(ZnPc) difference varies by up to 0.25 eV (cf. Fig. 2), i.e., being much larger than the experimental uncertainty of UPS (50 meV). Since the measured changes in V_{OC} are in the range of only 0.1 V, i.e., close to the experimental error of UPS, an independent and more precise technique than UPS is required to quantitatively resolve the causing weak variation in the effective gap. Therefore, FTPS measurements are performed which will be presented in the next section.

C. E_{CT} measurements

The UPS results are confirmed by measurements of the CT-state energy with Fourier-transform photocurrent spectroscopy (FTPS) on similar ZnPc:C_{60} BHJ solar cells. These samples consist of a layer sequence shown in the inset of Fig. 6. Here, the intrinsic C_{60} layer is omitted to avoid parasitic absorption during the FTPS measurements. Exchanging the *p*-doped HTL does not have any influence

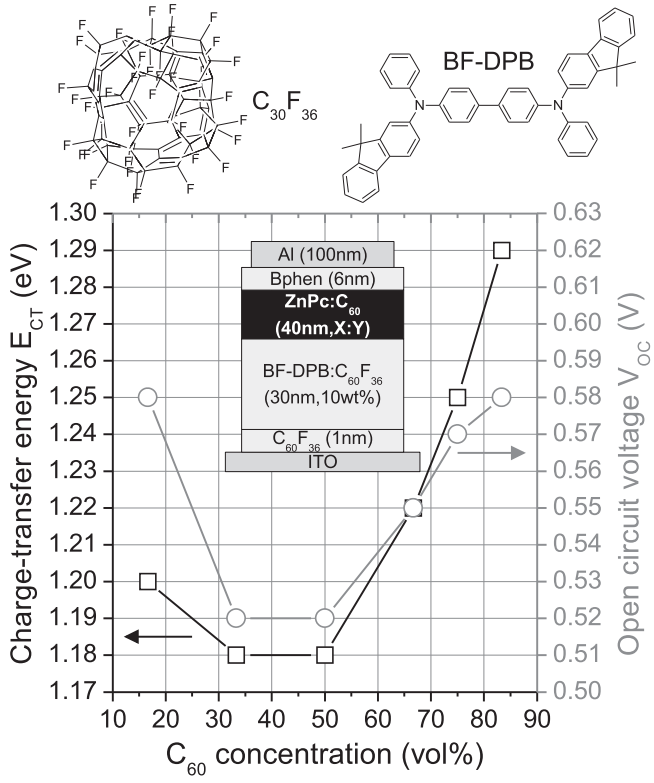

FIG. 6. Open-circuit voltage V_{OC} and charge-transfer energy E_{CT} of ZnPc:C_{60} pii-BHJ solar cells (inset) plotted versus the C_{60} concentration (mixing ratio varied from 5:1 to 1:5). The E_{CT} values are obtained by fitting the corresponding FTPS spectra (cf. Fig. 7).

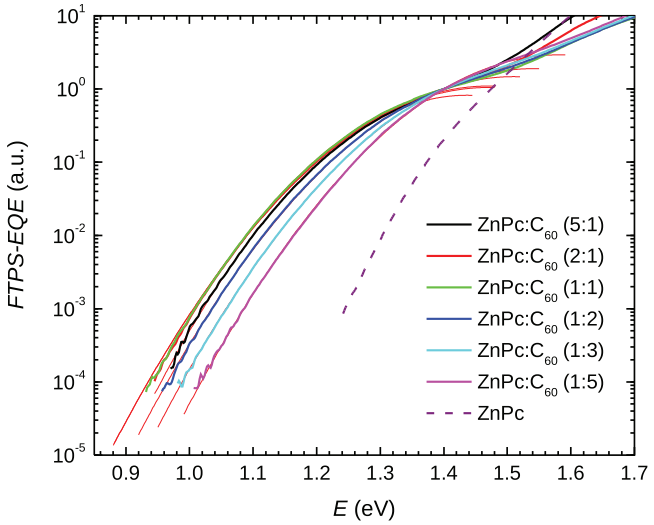

FIG. 7. (Color online) FTPS spectra of ZnPc:C_{60} pii-BHJ solar cells varying the mixing ratio from 1:5 to 5:1 (solid lines; device structure shown in the inset of Fig. 6). The red lines indicate the fit curves obtained by fitting the FTPS spectra with Eq. (2). The dashed line refers to a similar pii-FHJ solar cell containing only 50 nm ZnPc as photoactive layer.

on the active layer properties and V_{OC},[5] and hence on the CT-state energy E_{CT} of the ZnPc:C_{60} blends.

The measured FTPS spectra are normalized at 1.4 eV and shown in Fig. 7. Here, the ZnPc:C_{60} mixing ratio is varied from 5:1 to 1:5. The spectra are shifted to higher energies for rising C_{60} amounts and thus are indicating clearly an increase of the CT energy. The numerical values of E_{CT} are derived by fitting the FTPS spectra with Eq. (2) and the respective fit curves are indicated by red lines in Fig. 7. Hereby, the reorganization energy λ is in the range of 0.25 . . . 0.3 eV. The obtained E_{CT} values are plotted versus the C_{60} concentration together with V_{OC} in Fig. 6. The changes in the determined E_{CT} agree well with the trend in V_{OC}. The lowest E_{CT} value is observed at a C_{60} concentration of about 33 vol.% (2:1) and the highest value at 83 vol.% (1:5), which is approximately 0.1 eV higher. However, the absolute values of E_{CT} exceed eV_{OC} by more than 0.6 eV which must be related to several loss mechanisms, generally expressed by the device-specific parameter I_0 in Eq. (1). For the 17 vol.% (5:1) solar cell the relatively strong increase of V_{OC} is only qualitatively reproduced by the E_{CT} values. Here, an increase by only 20 meV is determined which will be discussed below. Nevertheless, the overall changes of the measured CT energies agree very well with the variations in the open-circuit voltages of the BHJ solar cells of Fig. 1.

The increase of V_{OC} for the 5:1 solar cell without the intrinsic C_{60} electron transport layer is much more pronounced than that for the corresponding device containing this layer (cf. Fig. 1). We attribute this difference to partly dissociation of excitons at the Bphen/ZnPc:C_{60}(5:1) interface, which gets significant only for the former type of solar cell and at the lowest C_{60} concentration. Due to the much lower EA of Bphen (EA $\approx$ 3.0 eV) compared to C_{60} (EA = 4.0 eV), the larger effective HOMO-LUMO gap of ZnPc/Bphen results in a higher achievable quasi-Fermi-level splitting at this interface. Indeed, a similar flat heterojunction (FHJ) solar cell consisting of ITO/$C_{60}F_{36}$(1 nm)/BF-DPB:$C_{60}F_{36}$ (30 nm, 10 wt.%)/ZnPc(50 nm)/Bphen(6 nm)/Al possesses an open-circuit voltage of V_{OC} = 0.76 V (j-V curve not shown here), i.e., $\approx$0.2 V more than measured for the ZnPc:C_{60} BHJ solar cells. Also the low-energy edge of the respective FTPS spectrum is shifted by $\approx$0.2 eV to higher energies (cf. Fig. 7, dashed line). Interestingly, at energies above 1.5 eV, FTPS features similar to the ZnPc/Bphen spectrum appear also for the ZnPc:C_{60} = 5:1 sample which is a strong hint on the high-energy contribution of the ZnPc/Bphen interface to V_{OC} in this device. However, this high-energy contribution is superimposed by the E_{CT} state of the ZnPc:C_{60} interface at lower energies, wherefore the determined E_{CT} value corresponds to the blend interface. Hence, the increase of eV_{OC} for the 17 vol.% (5:1) blend exceeds the determined CT-energy shift, because the latter only reflects the energy level changes within the blend, whereas the former additionally contains the high-energy contribution of the ZnPc/Bphen interface. For the BHJ solar cells containing the C_{60} transport layer (cf. Fig. 1) this contribution is not present, wherefore the changes in V_{OC} quantitatively agree very well with the shifts of E_{CT} determined from the cells without the interlayer.

Finally, the changes in the determined E_{CT} values upon blending ZnPc and C_{60} shall be compared to the ΔHOMO = HOMO(C_{60}) $-$ HOMO(ZnPc) differences measured by UPS [Fig. 3(b)]. Varying the mixing ratio from 25 vol.% (3:1) to 83 vol.% (1:6) yields a monotonous decrease of ΔHOMO by

0.19 eV, whereas the CT energy increases only by 0.11 eV. Furthermore, the slight increase of E_{CT} for the 14 vol.% (6:1) sample is not confirmed by the UPS measurements. The ΔHOMO difference decreases linearly for all measured blend ratios with increasing acceptor amount. Reasons for these deviations are the limited energy resolution of our UPS system (130 meV) as well as its experimental error regarding reproducibility (50 meV). However, the UPS data of Fig. 3 show a clear trend on the mixing ratio rather than a strong scattering, which is a strong hint on the reliability of the obtained data. More important might be changes of the individual electronic HOMO-LUMO gaps of C_{60} and ZnPc upon blending both materials. As indicated in Fig. 5, these changes could reach up to 0.15 eV (for C_{60}) although the optical gaps are shifting only by 0.018 eV (at least for ZnPc), i.e., being on the order of the variations in E_{CT} or eV_{OC}. However, the ΔHOMO values of the 1:6 (1.12 eV) and 6:1 (1.37 eV) samples even differ by 0.25 eV; i.e., the effective HOMO(ZnPc)-LUMO(C_{60}) gap could still change by 0.1 eV as observed for E_{CT}. Nevertheless, due to the low-resolution of IPES (400 meV), a change of the electronic gaps cannot be quantified sufficiently well enough for drawing clear conclusions on the origin of the deviations between the UPS and E_{CT} values. A possibility for the higher UPS values could be different experimental conditions. The CT energy spectra are measured during working conditions of complete solar cell stacks, i.e., under significant splitting of the quasi-Fermi-levels, whereas UPS is performed on single blend layers under UV illumination of much lower intensity than 1 sun, i.e., in equilibrium of the quasi-Fermi-levels.

However, although not precisely quantitatively specifiable, the observed V_{OC} dependence on the mixing ratio can be clearly attributed to changes in the energy levels of ZnPc and C_{60} due to mixing both materials. In the following sections, physical reasons for the observed energy level shifts and changes in E_{CT} will be discussed and examined by further experimental investigations.

D. Permittivity and XRD measurements

Two different explanations for the dependence of V_{OC} on the mixing ratio have been discussed in the literature for polymer-based donor:acceptor BHJ solar cells. On the one hand, a change of the average dielectric constant upon blending donor and acceptor materials at different ratios could lead to a stabilization or destabilization of the CT energy and a change in the IEs and EAs. For instance, for poly[2,7-(9,9-dialkylfluorene)-alt-5,5-(4,7-di-2-thienyl-2,1,3-benzothiadiazole)] (PF10TBT): [6,6]-phenyl-C61 butyric acid methyl ester (PCBM) BHJ solar cells a decrease of V_{OC} from 1.15 V to 1.00 V by increasing the PCBM concentration from 5 to 80 wt.% was reported.[8] There, the corresponding decrease of E_{CT} by ≈0.13 eV was explained by an increase of the effective blend permittivity from 3.4 (1 wt.% PCBM) to 3.85 (80 wt.% PCBM).[8] However, for the ZnPc:C_{60} BHJ solar cells the trend in V_{OC} is opposite (cf. Fig. 1). Therefore, measurements of the blend permittivity by impedance spectroscopy on metal/ZnPc:C_{60}(d nm)/metal structures are performed. Hereby, the blend thickness d is varied and the geometric capacitance of the device is plotted versus $1/d$ from which slope the relative permittivities ϵ_r are estimated. The obtained values are summarized in Table I. However, the results allow for no clear correlation with the observed trend in V_{OC} or E_{CT}. Interestingly, in accordance to the system PF10TBT:PCBM, the permittivity of the pure donor (ZnPc: 4.0) is lower than that of the pure acceptor (C_{60}: 5.0) layer, but the V_{OC} dependence on the acceptor concentration is inverse for both systems.

TABLE I. Relative permittivities ϵ_r of ZnPc:C_{60} blend layers with varied mixing ratios measured by impedance spectroscopy on metal/blend/metal structures.

C_{60} concentration (vol.%)	0	37	54	70	100
Relative permittivity ϵ_r	4.0	5.0	5.3	4.6	5.0

As a second reason, the energy-level shifts might be caused by morphological changes of the donor and/or acceptor phase due to blending both materials. For instance, increasing the fullerene amount in blends of poly[2-methoxy-5-(30,70-dimethyloctyloxy)-1,4-phenylene vinylene] (MDMO-PPV) and PCBM reduces E_{CT} by about 0.12 eV and hence also V_{OC}.[6] This trend was attributed to an increased phase separation and thus a rising amount of PCBM nanoclusters for high fullerene concentrations.[6] Also crystallization of the donor phase was reported to alter V_{OC}, e.g., for poly(3-hexylthiophene) (P3HT) and PCBM based solar cells.[21] Increasing the mass fraction of the well-defined highly crystalline polymer to the total polymer content from 10% to 90% leads to a decrease of V_{OC} by ≈0.11 V as well as of E_{CT} by 0.11 eV.[21] As well, for this polymer-based material system the V_{OC} dependence on the mixing ratio is inverse compared to the ZnPc:C_{60} blends investigated in the present article.

The morphology of ZnPc:C_{60} = 1:1 blends was already investigated by means of transmission and scanning electron microscopy (TEM, SEM),[22] grazing-incidence x-ray diffraction (GIXRD), variable-angle spectroscopic ellipsometry (VASE),[23] and atomic force microscopy (AFM).[22,23] An already phase-separated structure of both ZnPc and C_{60} domains was revealed by means of GIXRD for 1:1 blends evaporated at room temperature.[23] However, the crystallite sizes have to be very small (<10 nm) since the full width half maxima of the peaks in the GIXRD pattern are very broad. Similar results were also published for the small molecule system CuPc:C_{60}.[24]

In Fig. 8 GIXRD patterns of ZnPc:C_{60} blends with varied mixing ratios evaporated at room temperature are shown. Additionally, the diffraction pattern of pure ZnPc and C_{60} layers are plotted (dotted lines; cf. Ref. 23) to identify the obtained Bragg reflections. For the 6:1 blend (gray line) slightly broadened ZnPc peaks at $2\theta = \{7^\circ; 14^\circ\}$ are present. By increasing the fullerene concentration the ZnPc peaks are decreasing in intensity (due to lower donor amount in the blend) and get broadened, whereas C_{60}-related peaks arise at $2\theta = \{11^\circ; 18^\circ; 21^\circ\}$, but are strongly smeared out in comparison to the pure C_{60} film pattern. Only at the lowest ZnPc:C_{60} ratio of 1:6 (black line) distinct Bragg reflections of C_{60} are visible. Against that, already at a ZnPc:C_{60} ratio of 1:3 the C_{60} peaks at $2\theta = \{18^\circ; 21^\circ\}$ are significantly broadened which means that the formation of C_{60} crystals is strongly

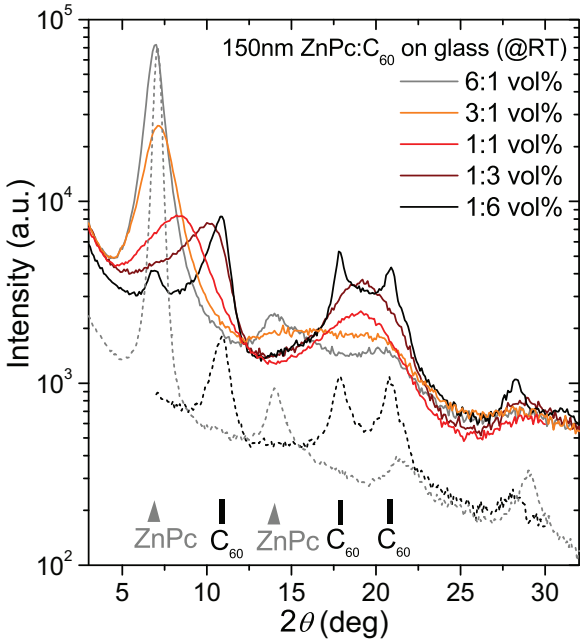

FIG. 8. (Color online) Grazing-incidence x-ray diffraction (GIXRD) spectra of ZnPc:C_{60} blends with varied mixing ratio thermally evaporated on glass at room temperature. The dotted lines indicate pure ZnPc (gray) or C_{60} (black) diffraction patterns.

disturbed by the presence of donor molecules. At medium concentrations, the peak at $2\theta = 11^\circ$ vanishes and finally no C_{60}-related peaks are visible for the ZnPc:C_{60} = 6:1 blend (gray line). For ZnPc the situation is different. Even at the highest acceptor concentration, the peak at $2\theta = 7^\circ$ is still present which indicates unambiguously a nano-crystalline ZnPc phase. At medium concentrations this peak is partly superimposed by the extremely broadened C_{60} features of the $2\theta = 11^\circ$ peak but clearly visible for concentrations above 1:1. However, in comparison to the pure ZnPc film, the $2\theta = 7^\circ$ peak is broadened for any mixing ratio which means significantly reduced crystal sizes within the blends. It shall be emphasized that although applying grazing-incidence XRD, the detection of the Bragg reflections is close to the resolution limit, and analyzing the samples by the usual specular XRD (Bragg-Bretano geometry) no features are detectable. This finding means that the actual crystal sizes of both materials remain in the range of only a few nanometers.[23] However, since a straightforward correlation of the GIXRD pattern with the UPS results is not possible, an even more extended quantitative analysis of the GIXRD peaks shall not be presented here and only qualitative conclusions will be sketched in the next paragraph.

In summary, we can learn from the GIXRD data that the ZnPc phase within the blend is mainly maintained nano-crystalline independent of the mixing ratio, whereas the C_{60} phase is significantly influenced by the amount of ZnPc molecules, and nanocrystallites are only present for fullerene concentrations above 75 vol.%. Also by UPS, the strongest shifts of the HOMO onsets with respect to the Fermi level as well as variations in the transport gap have been observed for C_{60} rather than for ZnPc [cf. Fig. 3(a)]. This comparison suggests a correlation between the morphology of the C_{60} phase and the respective energy levels, e.g., due to different strength of interactions between overlapping molecular orbitals in a nanocrystal or in a more disordered phase. For instance, all C_{60}-related GIXRD peaks disappear for the ZnPc:C_{60} = 6:1 sample; i.e., there seems to be an amorphous acceptor phase. In this case, the HOMO onset of C_{60} is shifted farthest from the ZnPc HOMO onset (cf. Fig. 2) which reduces the effective gap V_0 (and hence V_{OC}) to the lowest measured value. In contrast, for the 1:6 sample the C_{60} phase is nanocrystalline and the C_{60} HOMO onset is much closer to the ZnPc HOMO onset which increases V_0. Hence, the main driving force for the blend energy-level alignment and thus V_0 seems to be the crystallization grade of C_{60}.

E. Substrate dependence of the IE of ZnPc

Another explanation for the concentration dependence of the energy levels might be different growth modes of ZnPc. Investigating pure ZnPc layers by means of XRD, AFM, and VASE, Schünemann *et al.* showed that ZnPc grows in a standing-upright mode on weakly interacting substrates (glass, amorphous organics) due to Π-stacking of the flat ZnPc molecules (perpendicular to the substrate), whereas on strongly interacting surfaces (e.g., thermally evaporated gold on glass) the molecules are forced to lie almost flat.[25] Indeed, UPS measurements on 5 nm ZnPc films evaporated either directly on a (unoriented microcrystalline) gold foil or on top of an amorphous organic interlayer (e.g., *p*-doped MeO-TPD) reveal different IEs by more than 0.3 eV (corresponding UPS spectra are given in the Supplemental Material[18]). In the first case the IE is 5.31 eV, in the latter 4.98 eV. This difference must be attributed to the different orientations of ZnPc.

From the ZnPc:C_{60} blend UPS spectra, it is also possible to derive an individual IE value of ZnPc by IP(ZnPc) = Wf + HOMO-onset(ZnPc) (similarly for C_{60}), which is plotted in Fig. 3(d). It can be seen that with increasing C_{60} amount the IEs of ZnPc (gray triangles) as well as of C_{60} (black triangles) are increased by 0.13 eV and 0.27 eV, respectively. Hereby, the IE of ZnPc reaches 5.31 eV at high C_{60} concentrations (1:6 sample), which is interestingly equal to the increased IE observed for an intrinsic film evaporated on gold. In contrast, for high ZnPc amounts, the IE is 5.04 eV (3:1 sample), i.e., similar to intrinsic ZnPc on top of MeO-TPD. This comparison suggests that ZnPc molecules within blends might also orient with preferred directions depending on the mixing ratio. In particular at high C_{60} concentrations this would correspond to a growth mode similar to a pure film on gold. However, due to the small crystal sizes the ZnPc domains should be almost completely surrounded by C_{60} molecules in blends and the measured interface energetics should hence represent an average over all possible orientations without a preferred direction. For further clarification an even deeper general insight into the morphology of such donor-acceptor blends on a nanometer scale and the respective impact on the energetic landscape is necessary, but out of the scope of this article. Finally, we want to emphasize that for the blend layers only one clear HBEC arises in the UPS spectra, which is a strong hint for vacuum-level alignment between both species within and thus for the formation of a common blend work function. This fact is not self-evident, because for a flat ZnPc:C_{60} heterojunction a weak interface dipole was reported in the literature.[9]

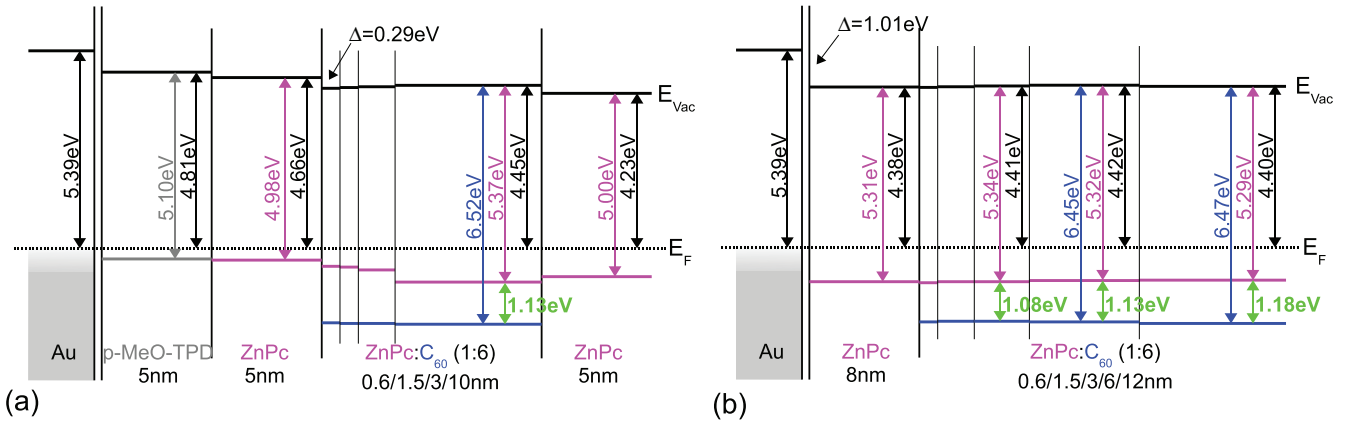

FIG. 9. (Color online) Level alignment of incrementally evaporated ZnPc:C_{60} blends (1:6, 0.6/1.5/3/10 nm) on either (a) Au/MeO-TPD:F6-TCNNQ (10 wt.%, 5 nm)/ZnPc (5 nm) or (b) Au/ZnPc (8 nm).

With the above findings it might be imaginable that the growth mode of ZnPc within blends and hence the energetic alignment is also influenced by the used gold substrate. Hence, it shall be finally shown that the observed level alignment of ZnPc and C_{60} (Fig. 3) is a general blend property and not influenced by the substrate or the growth mode of an underlaying ZnPc layer. Therefore, 1:6 blends are incrementally evaporated either on top of the Au/p-MeO-TPD/ZnPc or on the Au/ZnPc structure and investigated by UPS in comparison to the results obtained directly on gold (cf. Fig. 2). The resulting level alignments are summarized in Fig. 9. Whereas in the latter case the blend is evaporated on top of the "high IE" ZnPc, the first case represents an application of the ZnPc:C_{60} blend within a typical solar cell stack, i.e., on top of a HTL or a "low IE" ZnPc interlayer. In both cases the alignment results in the same HOMO(C_{60})-HOMO(ZnPc) difference of 1.13 eV after 3 nm. The same value was also obtained for the 1:6 blend evaporated directly on gold; i.e., the observed level shifts upon blending both materials are a general property of this BHJ. However, directly at the substrate/blend interface the alignment is determined by the properties of the substrate which results in higher [Fig. 9(a)] or lower [Fig. 9(b)] HOMO(C_{60})-HOMO(ZnPc) values. Nonetheless, after 3 nm the bulk properties of the blend are dominating which finally is more important for the achievable V_{OC} of a BHJ solar cell.

V. CONCLUSIONS

We have investigated the dependence of the open-circuit voltage of BHJ solar cells comprising ZnPc:C_{60} as active absorber blend on its mixing ratio. A linear increase of V_{OC} by 0.1 V has been found by increasing the C_{60} amount from 25 to 86 vol.%. The observed enhancement in V_{OC} is attributed to a respective increased effective donor-acceptor gap for high C_{60} concentrations which has been confirmed by UPS and IPES measurements. Furthermore, FTPS measurements reveal the same quantitative dependence of the energy of the charge-transfer state on the ZnPc:C_{60} mixing ratio as observed for V_{OC}. By using GIXRD a suppressed crystallization of the C_{60} phase by presence of donor molecules as well as different growth modes of the ZnPc phase are discussed as a physical origin for the changed energy levels within blend layers.

ACKNOWLEDGMENTS

The authors want to thank Lutz Wilde from the Fraunhofer CNT (Dresden, Germany) for performing the GIXRD measurements. This work was funded by the Deutsche Forschungsgemeinschaft and US National Science Foundation within the joint project "MatWorldNet" (Project Code LE 747/44-1). Work at Princeton was supported by the National Science Foundation (DMR-1005892).

*max.tietze@iapp.de
†Current address: Clarendon Laboratory, University of Oxford, Parks Road, Oxford OX1 3PU, England, UK.
‡leo@iapp.de
§Current address: Institut für Physikalische Chemie, Universität zu Köln, Luxemburger Straße 116, 50939 Köln, Germany.

[1]Heliatek press release, January 16, 2013; http://www.heliatek.com.
[2]G. Yu, J. Gao, J. C. Hummelen, F. Wudl, and A. J. Heeger, Science **270**, 1789 (1995).
[3]P. Peumanns, S. Uchida, and S. Forrest, Nature (London) **425**, 158 (2003).
[4]P. Wurfel, *Physics of Solar Cells* (Wiley-VCH, Weinheim, Germany, 2009).
[5]W. Tress, S. Pfützner, M. Riede, and K. Leo, J. Photon. Energy **1**, 011114 (2011).
[6]F. Piersimoni, S. Chambon, K. Vandewal, R. Mens, T. Boonen, A. Gadisa, M. Izquierdo, S. Filippone, B. Ruttens, J. D'Haen, N. Martin, L. Lutsen, D. Vanderzande, P. Adriaensens, and J. V. Manca, J. Phys. Chem. C **115**, 10873 (2011).
[7]F. C. Jamieson, E. B. Domingo, T. McCarthy-Ward, M. Heeney, N. Stingelin, and J. R. Durrant, Chem. Sci. **3**, 485 (2012).

[8]D. Veldmann, Ö. Ipek, S. C. J. Meskers, J. Sweelssen, M. M. Koetse, S. C. Veenstra, J. M. Kroon, S. S. van Bavel, J. Loos, and R. A. J. Janssen, J. Am. Chem. Soc. **130**, 7721 (2008).
[9]S. H. Park, J. G. Jeong, H.-J. Kim, S.-H. Park, M.-H. Cho, S. W. Cho, Y. Yi, M. Y. Heo, and H. Sohn, Appl. Phys. Lett. **96**, 013302 (2010).
[10]W. Tress, K. Leo, and M. Riede, Adv. Funct. Mater. **21**, 2140 (2011).
[11]G. Garcia-Belmonte, Sol. Energy Mater. Sol. Cells **94**, 2166 (2010).
[12]B. P. Rand, D. P. Burk, and S. R. Forrest, Phys. Rev. B **75**, 115327 (2007).
[13]A. Wilke, J. Endres, U. Hörmann, J. Niederhausen, R. Schlesinger, J. Frisch, P. Amsalem, J. Wagner, M. Gruber, A. Opitz, A. Vollmer, W. Brütting, A. Kahn, and N. Koch, Appl. Phys. Lett. **101**, 233301 (2012).
[14]J. Widmer, M. Tietze, K. Leo, and M. Riede, Adv. Funct. Mater. (2013), doi: 10.1002/adfm.201301048.
[15]K. Vandewal, K. Tvingstedt, A. Gadisa, O. Inganas, and J. V. Manca, Phys. Rev. B **81**, 125204 (2010).
[16]C. I. Wu, Y. Hirose, H. Sirringhaus, and A. Kahn, Chem. Phys. Lett. **272**, 43 (1997).
[17]C. Elschner, A. A. Levin, L. Wilde, J. Grenzer, C. Schroer, K. Leo, and M. Riede, J. Appl. Crystallogr. **44**, 983 (2011).
[18]See Supplemental Material at http://link.aps.org/supplemental/10.1103/PhysRevB.88.085119 for the variation of the fill-factor, short-circuit current and the power conversion efficiency versus the blend mixing ratio of the solar cells of Fig. 1. Additionally, UPS spectra of the samples of Fig. 9 are given.
[19]W. Tress, A. Merten, M. Furno, M. Hein, K. Leo, and M. Riede, Adv. Energy Mater. **3**, 631 (2013).
[20]W. Zhao and A. Kahn, J. Appl. Phys. **105**, 123711 (2009).
[21]K. Vandewal, W. D. Oosterbaan, S. Bertho, V. Vrindts, A. Gadisa, L. Lutsen, D. Vanderzande, and J. V. Manca, Appl. Phys. Lett. **95**, 123303 (2009).
[22]S. Pfützner, C. Mickel, J. Jankowski, M. Hein, J. Meiss, C. Schünemann, C. Elschner, A. A. Levin, B. Rellinghaus, K. Leo, and M. Riede, Org. Electron. **12**, 435 (2011).
[23]C. Schünemann, D. Wynands, L. Wilde, M. P. Hein, S. Pfützner, C. Elschner, K.-J. Eichhorn, K. Leo, and M. Riede, Phys. Rev. B **85**, 245314 (2012).
[24]B. P. Rand, J. Xue, S. Uchida, and S. F. Forrest, J. Appl. Phys. **98**, 124902 (2005).
[25]C. Schünemann, D. Wynands, K.-J. Eichhorn, M. Stamm, K. Leo, and M. Riede, J. Phys. Chem. C **117**, 11600 (2013).